Neoplasma 2024; 71(5): 451–462

doi:10.4149/neo_2024_240511N214

Six2 regulates the malignant progression and 5-FU resistance of hepatocellular carcinoma through the PI3K/AKT/mTOR pathway and DNMT1/E-cadherin methylation mechanism

Jianwang LI[1,*], Xiaozhen CHENG[1], Denggao HUANG[2], Ronghua CUI[1]

[1]Department of Oncology, Xiangya School of Medicine Affiliated Haikou Hospital, Haikou People's Hospital, Haikou, Hainan, China; [2]Department of Central Laboratory, Xiangya School of Medicine Affiliated Haikou Hospital, Haikou People's Hospital, Haikou, Hainan, China

**Correspondence: ljw7505@163.com*

Received May 11, 2024 / Accepted October 8, 2024

This study focuses on exploring the role of Six2 in the progression of hepatocellular carcinoma (HCC) and its resistance to the chemotherapy drug 5-fluorouracil (5-FU). Using Hep3B and Huh7 cell lines, we analyzed how Six2 affects various cellular functions, including viability, proliferation, apoptosis, and invasion. Our research also delved into Six2's regulatory impact on DNMT1 levels, E-cadherin expression, and the methylation of the E-cadherin promoter, all of which are crucial for 5-FU resistance in HCC cells. Additionally, we examined the effects of Six2 knockdown on the PI3K/AKT/mTOR signaling pathway. Our findings indicate that overexpression of Six2 enhances cell viability and proliferation, encourages invasive behavior, increases methylation at the E-cadherin promoter, and reduces apoptosis. These changes correspond with increased levels of DNMT1 and decreased levels of E-cadherin, culminating in heightened resistance to 5-FU. Conversely, knocking down Six2 increases the sensitivity of HCC cells to 5-FU and reduces activation of the PI3K/AKT/mTOR pathway. These results suggest that Six2 plays a significant role in promoting HCC proliferation, invasion, and chemotherapy resistance, particularly through mechanisms involving DNMT1 and the PI3K/AKT/mTOR pathway, highlighting its potential as a target for HCC treatment.

Key words: hepatocellular carcinoma; E-cadherin; methylation; Six2; 5-FU resistance

Liver cancer is a prevalent malignancy globally, with approximately 841,000 new cases reported annually [1]. Hepatocellular carcinoma (HCC), the primary form of liver cancer, ranks as the sixth most common cancer worldwide [2]. Early-stage HCC is typically asymptomatic, which often leads to delayed diagnosis and presentation at an advanced stage, precluding curative surgical intervention as with pancreatic cancer [3]. Thus, surgical resection, adjuvant radiotherapy, and comprehensive therapy are the primary treatments for HCC at present [4]. However, the highly aggressive nature and high recurrence rate of HCC result in a significant mortality rate of up to 8.2% [5, 6]. For advanced, unresectable HCC, chemotherapy with 5-fluorouracil (5-FU) is occasionally selected [7]. However, the therapeutic efficacy of 5-FU is not entirely satisfactory, necessitating further exploration of its mechanism to enhance its therapeutic outcomes. *Six2* (*SIX homeobox 2*, gene ID: 10736) encodes a homeodomain transcription factor and has been confirmed to be critical for embryonic growth and differentiation [8–10]. Additionally, *Six2* regulates both the proliferation (self-renewal) and differentiation of nephron progenitor cells during kidney organogenesis [11]. Gene expression pattern and cellular processes that regulate the process of embryogenesis and embryonic development frequently play crucial roles in tumorigenesis [12, 13]. Therefore, it is not surprising that *Six2* is frequently aberrantly activated in tumors. *Six2* is intricately involved in the pathogenesis and progression of several malignancies, such as colorectal cancer (CRC) [14], Wilms' tumor [15], and clear cell renal cell carcinoma [16]. Our previous investigations revealed a strong correlation between elevated Six2 expression in HCC with poor prognosis and decreased sensitivity to 5-FU therapy [4]. However, its molecular mechanisms and functions *in vivo* are not yet fully understood. Furthermore, recent research has uncovered the role of Six2 in promoting epithelial-mesenchymal transition (EMT) in HCC [17].

E-cadherin, the epithelial marker of EMT, acts as a tumor suppressor via inhibiting tumor metastasis and enhancing stemness [18]. We demonstrated that Six2 negatively modulates E-cadherin levels by promoting its promoter methylation in HCC, a finding later confirmed in non-small cell lung cancer [4, 19]. Methylation of DNA occurs when a cytosine residue is methylated within a cytosine-phosphate-guanine (CpG) site [20]. Genomic DNA in mammals is mainly methylated by DNA methyltransferases, including DNMT1, DNMT3α, and DNMT3β [21]. The research indicates that targeting the PI3K/Akt/mTOR pathway may represent a promising therapeutic approach for HCC [22]. In this study, we primarily investigated the role of Six2 in HCC cell proliferation, invasion, and resistance to 5-FU, as well as the underlying molecular mechanisms related to E-cadherin expression and the PI3K/Akt/mTOR signaling pathway. Elucidating these aspects is crucial for a comprehensive understanding of HCC pathogenesis and contributes to the development of innovative and potent therapeutic targets for HCC.

Materials and methods

Cell culture. The liver cancer cell lines Hep3B and Huh7 were procured from the Chinese Academy of Sciences. Cells were maintained in a 37 °C incubator with 5% CO_2. Hep3B and Huh7 cells were kept in DMEM medium (cat. no.12430054, Gibco), which contained 10% FBS (cat. no.10100147, Gibco) and 1% penicillin/streptomycin (cat. no.15070063, Gibco). Cells were treated with 5-FU (cat # S1209, Selleck) at final concentrations of 0 μM, 6 μM, and 9 μM for 24 h [23]. SC79 (SF2730, Beyotime) was applied at a final concentration of 8 μg/ml for 24 h according to the manufacturer's instructions.

Quantitative real-time polymerase chain reaction (qPCR). To extract total RNA, 1 ml of TRIzol (cat. no. R1030, Beijing Applygen Technologies Inc.) was added to the cell pellet of the sample to enable effective cell lysis and RNA separation. Then, the quality of the extracted RNA was measured using a NanoDrop 2000. Next, RNA was reversely transcribed into cDNA by utilizing a Promega M-MLV kit (cat. no. M1705), which facilitates downstream quantitative PCR. KAPA SYBR FAST qPCR kit (Kapa Biosystems) was utilized as the quantitative PCR reaction system, in conjunction with SimpliAmp™ PCR System, to determine the relative mRNA expression. Six2 upstream primer: GCACAACCCCTACCCTTCAC, downstream primer: TCTCGTTGTTCTCCCTTTCCTT; DNMT1 upstream primer: CCGACTACATCAAAGGCAGC, downstream primer: AGGTTGATGTCTGCGTGGTA; E-cadherin upstream primer: ATTTTTCCCTCGACACCCGAT, downstream primer: TCCCAGGCGTAGACCAAGA; GAPDH upstream primer: CCAGGTGGTCTCCTCTGA, downstream primer: GCTGTAGCCAAATTCGTTG.

Western blot. Protein quantification in liver cancer cell lines and hepatocytes was performed using the BCA method (cat. no. 23225, Thermo Fisher). Subsequently, 5 μg of protein was separated using 2× SDS sample buffer on 12% SDS-acrylamide gels, followed by a transfer onto PVDF membranes. These membranes were incubated for 12 h with primary antibodies against Six2 (18596, 1:1000, CST), DNMT1 (5032, 1:1000, CST), E-cadherin (14472, 1:1000, CST), mTOR (ab134903, 1:10000, Abcam), AKT (60203-2-Ig, 1:5000, Proteintech), PI3K (20584-1-AP, 1:1000, Proteintech), p-mTOR (ab109268, 1:1000, Abcam), p-AKT (66444-1-Ig, 1:5000, Proteintech), p-PI3K (ab278545, 0.5 μg, Abcam), GADPH (ab8245, 1:1000, Abcam), and β-actin (60009-1-Ig, 1:1000; Proteintech) in the presence of 5% non-fat milk, followed by the incubation with secondary antibodies conjugated with horseradish peroxidase. The immunoreactive bands were detected using a specific ECL kit (P0018S, Beyotime) and an Odyssey Scanning System.

Immunofluorescence. Cells were plated in a 35 mm dish suitable for confocal microscopy and cultured for 48 h. They were then fixed with 4% paraformaldehyde for 20 min, followed by permeabilization with 0.5% Triton X-100 for 20 min, and then blocked with 3% BSA for 1 h. After overnight incubation at 4 °C with anti-Six2, anti-DNMT1, or anti-E-cadherin antibody, cells were treated with fluorescein-conjugated secondary antibodies (cat. no. A28175 and A27039, ThermoFisher Scientific) for 2 h. The cells were stained with DAPI (cat. no. D1306, ThermoFisher Scientific) for 10 min before being observed with a Carl Zeiss LSM 510 META confocal microscope.

Vector construction and lentiviral infection. We commissioned Anernor Inc (Guangzhou, China) to construct lentiviral vectors (LV3) for Six2 overexpression (OE-Six2, GeneBank ID: NM_016932.5) and Six2 knockdown (KD-Six2), which were confirmed by DNA sequencing. Hep3B and Huh7 cells were transduced with lentiviral vectors at an MOI of 10, followed by the collection of the transduced cells 96 h post-transduction for assessment of transduction efficiency via qPCR and western blot. The knockdown sequence design was as follows: KD1- Six2: GCGAGCACCTTCACAAGAATG; KD2- Six2: GCACCTTCACAAGAATGAAAG; KD3- Six2: ACAAGATCCTGGAGAGCCACC; KD-NC: TTCTCCGAACGTGTCACGT.

CCK-8 assay. Hep3B and Huh7 cells were seeded in 96 well plates and incubated for a period of 5 consecutive days in a CO_2 incubator maintained at 37 °C. Following this, each well was treated with 10 μl of CCK-8 reagent (cat. no. 96992, St. Louis, MO, USA) and incubated for 3 h before measuring the OD values at 450 nm via a Spectrafluor microreader plate (Molecular Devices, LLC). The aforementioned experimental protocol was replicated three times for the sake of validating the results.

The half-maximal inhibitory concentration (IC_{50}) assay. The Hep3B and Huh7 cells were seeded into 96-well plates at an appropriate density and incubated at 37 °C in a humidified atmosphere with 5% CO_2 for 24 h. After attachment, the cells were treated with various concentrations of 5-FU (0,

2, 4, 8, 16, 32, and 64 μM) and incubated for an additional 24 h. Following drug treatment, 10 μl of CCK-8 reagent (cat. no. 96992, St. Louis, MO, USA) was added to each well and incubated for 3 h. The absorbance at 450 nm was measured using a microplate reader (Spectrafluor, Molecular Devices, LLC). Cell viability inhibition was calculated as a percentage relative to the untreated control group. IC_{50} of 5-FU was determined using non-linear regression analysis performed with GraphPad Prism software (v9.0). Each experiment was repeated three times independently to ensure reproducibility of the results.

Colony formation assay. Hep3B and Huh7 cell lines were seeded in 6-well plates. The medium was replaced every 3 days, followed by regular observation of the cell growth. After 14 days, each well was fixed with 4% paraformaldehyde (1 ml) for 45 min. Subsequently, cells were washed once with PBS, followed by staining with 500 μl GIEMSA dye solution for 20 min. We enumerated the number of discernible colonies through visual inspection.

Apoptosis analysis. To determine the apoptotic fractions of Hep3B and Huh7 cells, Annexin V and PI staining was performed via a commercial kit (cat. no. V13241; Thermo Fisher Scientific). Following two PBS washes, cells were centrifuged at 300×g for 5 min. The resultant pellet was suspended in 195 μl of Annexin V-FITC/PI binding buffer, which was subsequently supplemented with 5 μl of Annexin V-FITC and 10 μl of PI. The cells were incubated in the dark for 30 min, then washed and suspended for flow cytometric (CytoFLEX; BECKMAN) analysis to evaluate apoptosis. The minimum event count per sample was set to 10,000, and acquisition stopped when the sample volume was depleted.

Wound healing assay. Specifically, 1×10^5 cells/well were seeded in 24-well culture plates with a confluence of approximately 90%. Next, a scratch was created using a scratcher (cat. no. VP408FH, VP Scientific, Inc.), followed by rinsing each well three times with PBS. Scratch pictures were captured at 0, 24, and 48 h. ImageJ software was used to quantify the width of the gap. The healing rate was calculated: (healing area at 0 h – healing area at 24/48 h) / healing area at 0 h.

Cell invasion assay. The invasion ability of Hep3B and Huh7 cells was assessed using a Transwell kit (cat. no. 3422; Corning). Specifically, 100 μl of diluted Matrigel was added to the top chamber and allowed to solidify at 37 °C. Then, 5×10^4 cells were added to the top chamber, while 0.5 ml 30% FBS medium was added to the bottom chamber. Following a 48 h incubation period at 37 °C, the invaded cells on the bottom chamber were stained using 0.5% crystal violet 0.5 h, followed by rinsing the chamber with PBS. Subsequently, images of six random fields per group were captured via a microscope (Leica Camera AG).

Primers for bisulfite sequencing PCR (BSP). BSP primers targeting the promoter region of the E-cadherin gene were designed by retrieving the sequence from the UCSC database (https://genome-asia.ucsc.edu/) and inputting it into the MethPrimer software. Following preliminary experiments with multiple primer pairs, the sequences of the chosen primers were established: forward primer (BSP-F): TTTAGTAATTTTAGGTTAGAGGGTTAT, and reverse primer (BSP-R): AAACTCACAAATACTTTACAATTCC. DNA extraction was performed using the TIANamp Genomic DNA Kit from Tiangen Biotech. After extraction, the genomic DNA (3 μg) was diluted to 50 μl with nuclease-free water and treated with NaOH to a final concentration of 0.2 M for denaturation at 42 °C for 30 min. This was followed by the addition of 30 μl of 10 mM hydroquinone and 520 μl of 3 M sodium bisulfite (pH 5.0), gently mixed and then overlaid with 200 μl of mineral oil to prevent evaporation and oxidation. The mixture was incubated at 50 °C in the dark for 16 h. The bisulfite-modified DNA was then purified using a column purification kit and eluted in 50 μl of nuclease-free water to determine the DNA concentration. For PCR amplification, an optimized reaction system was employed with a total volume of 50 μl, comprising 0.25 μl TaKaRa EpiTaq HS (5 U/μl), 5 μl 10× EpiTaq PCR Buffer (Mg^{2+} free), 5 μl 25 mM $MgCl_2$, 100 ng of bisulfite-treated DNA template, 20 pmol of each primer (F and R), 4 μl of dNTP mix (each 2.5 mM), and sterile water up to volume. The PCR program consisted of an initial denaturation at 98 °C for 2 min, followed by 35 cycles of 98 °C for 10 s, 55 °C for 30 s, and 72 °C for 30 s, with a final extension at 72 °C for 2 min. The amplified products were separated by agarose gel electrophoresis, and the gel slices containing the target DNA fragments were excised and subjected to a gel recovery step. The recovered amplification fragments were then ligated into the T-vector for cloning. The clones were identified through colony PCR and sequencing to ensure a minimum of 5 valid sequencing datasets for each sample. Finally, data analysis and graphical representation were conducted to present and interpret the experimental results.

Methylation-specific PCR (MSP). The DNA samples underwent bisulfite conversion using the QIAamp EpiTect Fast DNA Bisulfite kit (QIAGEN, cat. no. 59824). E-cadherin methylation forward primer: GGTTGGGTAATATAGGGAGATATAGC; reverse primer: TCGAACTCCTAAACTCAAACGAT. E-cadherin unmethylation upstream primer: TGGGTAATATAGGGAGATATAGTGT, downstream primer: CCTCAAACTCCTAAACTCAAACAAT.

Chromatin immunoprecipitation (ChIP). The Pierce Magnetic ChIP Kit (cat. no. 26157, ThermoFisher Scientific) was used to perform ChIP. In brief, 2×10^6 cells were cross-linked with formaldehyde, harvested, and then subjected to MNase treatment and sonication. DNMT1 antibody was added, and Protein A and G conjugated magnetic beads were used to recover the protein-chromatin complex. Real-time PCR was performed on eluted DNA using E-cadherin promoter-specific primers (forward: 5'-GGGAGTCCCACAACAGCATA-3'; reverse: 5'-TTCCCTAGGTCAGGACCACC-3'). Subsequently, agarose gel electrophoresis was conducted, and images were acquired using a Tanon 1600 Gel Image Processing System.

***In vivo* experiments in nude mice.** All animal experiments were conducted in compliance with the ARRIVE 2.0 guidelines [24] and should comply with the U.K. Animals (Scientific Procedures) Act, 1986, and associated guidelines [25]. Efforts were made to minimize the number of animals used and to mitigate their suffering in line with these guidelines. Nude mice purchased from Hunan Slake Jingda Experimental Animal Co., Ltd, eighteen male BALB/c nude mice aged 6–8 weeks, were divided into three groups, with housing randomized across different cage locations to control for environmental factors. Each group received injections of Huh7 cells, with six mice per group. Cells were prepared into cell suspensions after 96 h post-culture, and 100 µl containing 1×10^6 cells were subcutaneously injected into the right dorsal side of the nude mice [26]. Tumor length and width were measured every three days using calipers. Tumor volume was calculated and recorded according to the formula: Volume = Length × Width^2 × 0.52. When tumor volumes reached 20 mm^3, which typically occurred around day 7, mice were intravenously injected with 100 µl of 5-FU (500 mg/kg/mouse/day) via the tail vein for seven consecutive days [27]. Mice were sacrificed on day 15 through cervical dislocation following anesthesia (lidocaine, 4 mg/kg, intraperitoneal injection). Tumors were then photographed and categorized according to their respective groups.

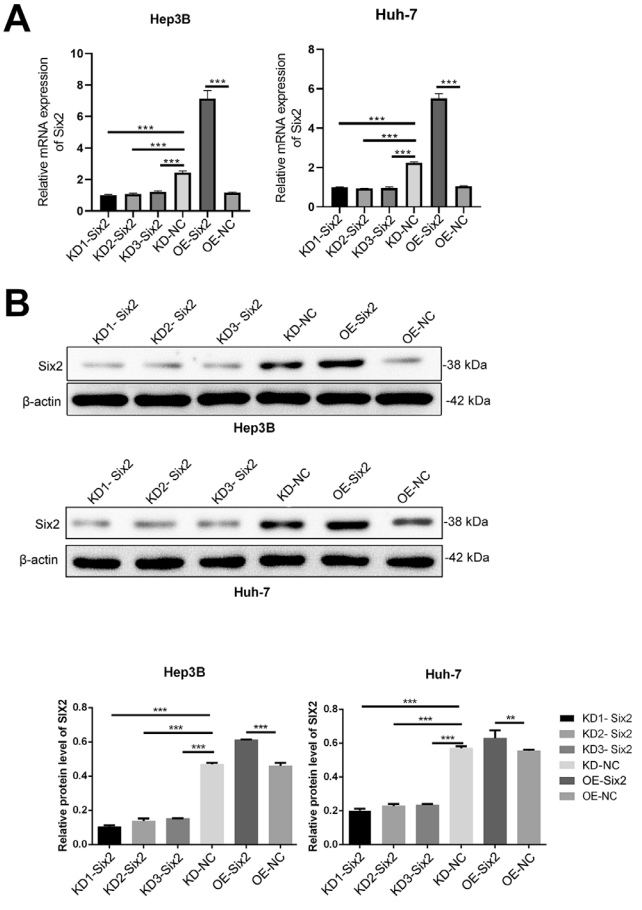

Figure 1. Successfully constructed Six2-overexpressing and -silenced HCC cells. Transfection efficiency of Six2 knockdown and overexpression lentivirus assessed by qPCR (A) and western blot (B). Grayscale analysis was conducted using ImageJ software. All experiments were performed with three biological replicates. Means ± SD **p<0.01, ***p<0.001.

Ethical statement. This study was approved by the Ethics Committee of Haikou People's Hospital, located in Haikou, Hainan, China (Approval number: 2019-(Lunshen-016). All animal experiments were conducted in compliance with the ARRIVE guidelines and should be carried out in accordance with the U.K. Animals (Scientific Procedures) Act, 1986, and associated guidelines.

Statistical analysis. The normality of distribution was assessed using Kolmogorov-Smirnov testing to determine whether variables were parametric or nonparametric. Parametric comparisons between two groups were performed using an unpaired Student's t-test, while multiple parametric comparisons were conducted using one-way ANOVA followed by Tukey's post hoc test. Nonparametric variables were analyzed using Mann-Whitney U testing. A p-value less than 0.05 was considered statistically significant.

Results

Successfully constructed *Six2* overexpressing and silenced HCC cells. In our prior investigation, we validated that heightened Six2 expression led to reduced E-cadherin expression through promoter methylation, specifically in HCC [28]. To investigate Six2's role in HCC, we utilized lentivirus-mediated knockdown and overexpression in Hep3B and Huh7 cells, confirming transfection efficiency via qPCR and western blot analysis. The results indicated that we successfully silenced and overexpressed *Six2* in Hep3B and Huh7 cells (Figures 1A, 1B).

***Six2* promoted the progression of HCC cells.** Upregulation of *Six2* increased the viability of HCC cells, while silencing of *Six2* markedly suppressed viability in both Hep3B and Huh7 cells (Figure 2A). Furthermore, overexpression of *Six2* dramatically enhanced the proliferation rate of Huh7 and Hep3B cells, whereas knockdown of *Six2* resulted in a significant reduction of proliferation rate (Figure 2B). To further estimate the Six2 effect on apoptosis in HCC cells, flow cytometry assays were conducted. The results showed that overexpression of Six2 pronouncedly reduced the apoptosis rate of Hep3B and Huh7 cells, whereas silencing of Six2 significantly promoted apoptosis (Figure 2C). The scratch assay revealed that the overexpression of Six2 contributed to a significant reduction in scratch width with an increase in healing rate on Huh7 and Hep3B cells, whereas Six2 silencing led to a notable widening of scratch width and a decrease in healing rate 48 h post-scratching (Figure 3A). Furthermore, the upregulation of Six2 remarkably enhanced cell invasion in Hep3B and Huh7 cells, while its knockdown significantly impeded invasion (Figure 3B).

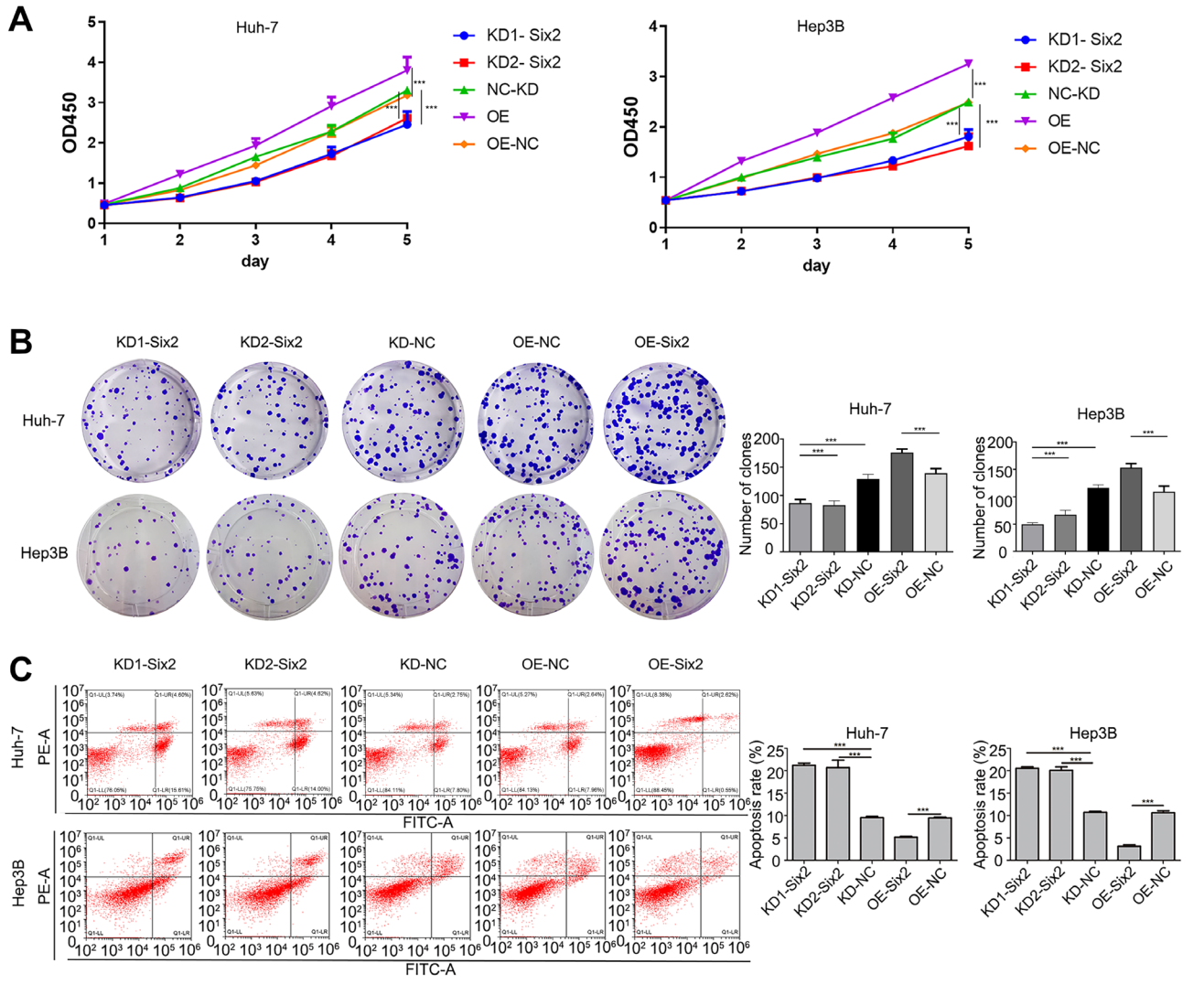

Figure 2. Six2 promoted the growth and proliferation of HCC cells. Hep3B and Huh7 cells were transfected with Six2-knockdown and -overexpression lentivirus vectors. A) The viability of Hep3B and Huh7 cells was detected by CCK-8 assay. B) The proliferation ability of Hep3B and Huh7 cells was determined by colony formation assay. C) Representative dot plots of cell apoptosis in Hep3B and Huh7 cells. All experiments were performed with three biological replicates. Means ± SD ***p<0.001.

Six2 promoted the promoter methylation of E-cadherin by targeting DNMT1. This study explored the effect of Six2 on the expression of DNMT1 and E-cadherin in HCC cells. Overexpression of Six2 significantly increased DNMT1 expression, whereas its silencing decreased DNMT1 expression in Hep3B and Huh7 cells (Figures 4A, 4B). Conversely, E-cadherin expression was notably reduced in response to Six2 overexpression but markedly increased upon Six2 silencing in both cell lines (Figures 4A, 4B). Furthermore, we examined the alterations in DNA methylation levels within the E-cadherin promoter region using BSP and MSP assays in Huh7 cells transfected with Six2-knockdown and -overexpression lentivirus. CG pairs within the E-cadherin promoter region were substantially hypomethylated in Six2-knockdown Huh7 cells, whereas they were hypermethylated in Six2-overexpression Huh7 cells (Figures 4C, 4D). Moreover, we evaluated the *in vitro* relevance of DNMT1 binding to the E-cadherin promoter regulated by Six2 via the ChIP assays. Notably, we observed a decrease in DNMT1 binding in response to Six2 knockdown in the E-cadherin promoter (Figure 4E).

Six2 overexpression enhances resistance to 5-FU in HCC cells. After transfecting Huh7 and Hep3B cells with Six2-overexpression and negative control vectors, we treated them with 5-FU at concentrations of 0 μM, 6 μM, and 9 μM. Results from the colony formation assay revealed that the number of colonies in the Six2-overexpression group was significantly higher than that in the negative control vector

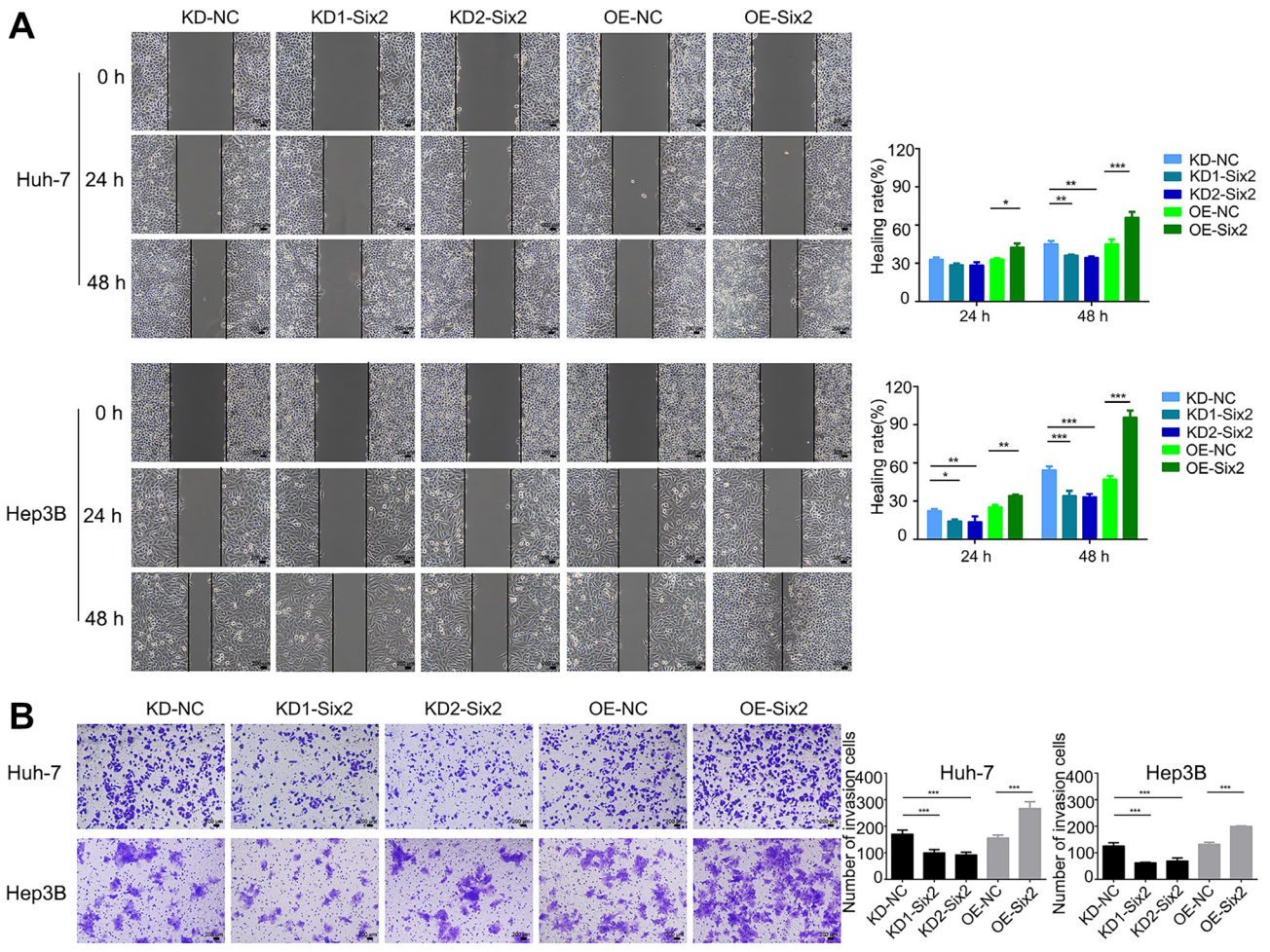

Figure 3. Six2 accelerated the migration and invasion of HCC cells. Hep3B and Huh7 cells were transfected with Six2-knockdown and -overexpression lentivirus vectors. A) The migration ability of Hep3B and Huh7 cells was detected by scratch experiments. B) The invasion ability of Hep3B and Huh7 cells was evaluated by the Transwell invasion assay. All experiments were performed with three biological replicates. Means ± SD *p<0.05, **p<0.01, ***p<0.001.

group (OE-NC) under 0 μM, 6 μM, and 9 μM 5-FU treatments (Figure 5A). Flow cytometry assays revealed that the apoptosis rate in the Six2-overexpression group was significantly lower than in the OE-NC group across all 5-FU treatments (Figure 5B). These findings suggest that Six2 overexpression augments resistance to 5-FU in Huh7 and Hep3B HCC cells. The IC_{50} assay results demonstrated that in both Huh7 and Hep3B cells, the IC_{50} values of the Six2-overexpression group were significantly higher than those of the OE-NC group (Figure 5C), indicating that Six2 overexpression significantly reduced the inhibitory effect of 5-FU on cell proliferation.

Inhibition of Six2 expression enhances the effect of combined Six2 knockdown and 5-FU treatment on HCC cells in nude mice. Xenograft studies showed that tumor volume was significantly reduced in the two Six2-silenced groups (KD1-Six2+5-FU and KD2-Six2+5-FU) compared to the negative control group (NC-KD+5-FU) (Figure 6). These findings suggest that Six2 knockdown may enhance the inhibitory effect of 5-FU on HCC cells *in vivo*.

Six2 knockdown inhibits HCC cell proliferation and invasion by suppressing the PI3K/Akt/mTOR pathway. Western blot analyses showed that Six2 silencing (KD1-Six2 and KD2-Six2) significantly reduced the expression of p-AKT/AKT, p-PI3K/PI3K, and p-mTOR/mTOR proteins in Huh7 and Hep3B cells, compared to the negative control group (NC-KD) (Figure 7A). Additionally, SC79 (an Akt activator) was able to reverse the inhibitory effect on colony formation (Figure 7B) and the number of invasive cells (Figure 7C) induced by Six2 silencing.

Discussion

Despite substantial advancements in understanding HCC molecular and signaling pathways, effective early diagnostic methods and targeted therapies for this disease

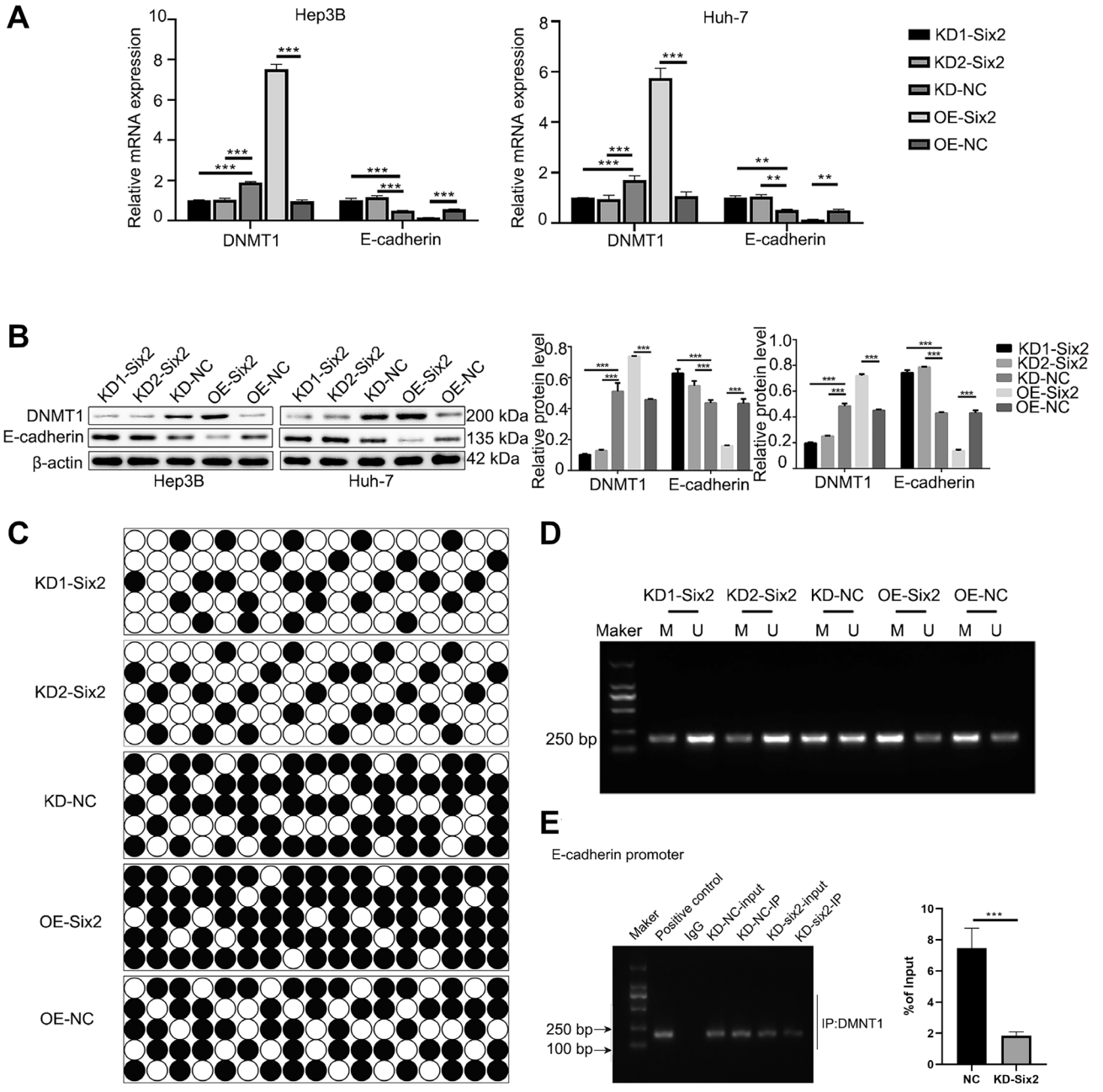

Figure 4. Six2 promoted methylation of the E-cadherin promoter via stimulating DNMT1. Hep3B and Huh7 cells were transfected with Six2-knockdown and -overexpression lentivirus vectors. A, B) The mRNA and protein levels of DNMT1 and E-cadherin in Hep3B and Huh7 cells were determined via qPCR (A) and western blot (B). Grayscale analysis was performed by ImageJ software. C, D) DNA methylation level of E-cadherin promoter in Huh7 cells was measured by BSP (C) and MSP (D). E) ChIP assay was conducted to evaluate DNMT1 binding to putative binding sites on the E-cadherin gene promoter regions. All experiments were performed with three biological replicates. Means ± SD **p<0.01, ***p<0.001.

remain limited. Consequently, the incidence and mortality rates associated with HCC continue to rise annually. [6] The combined regimen of 5-FU and oxaliplatin has long been considered the standard treatment for CRC and HCC. However, drug resistance observed in a subset of patients limits its therapeutic efficacy [29].

Initially, *Six2* was demonstrated to function in a cell-autonomous manner and was associated with regulating a multipotent self-renewing nephron progenitor population crucial for the entire process of kidney development [30, 31]. Notably, deficiency of Six2 during fetal development has been linked to chronic renal failure, elevated blood pressure,

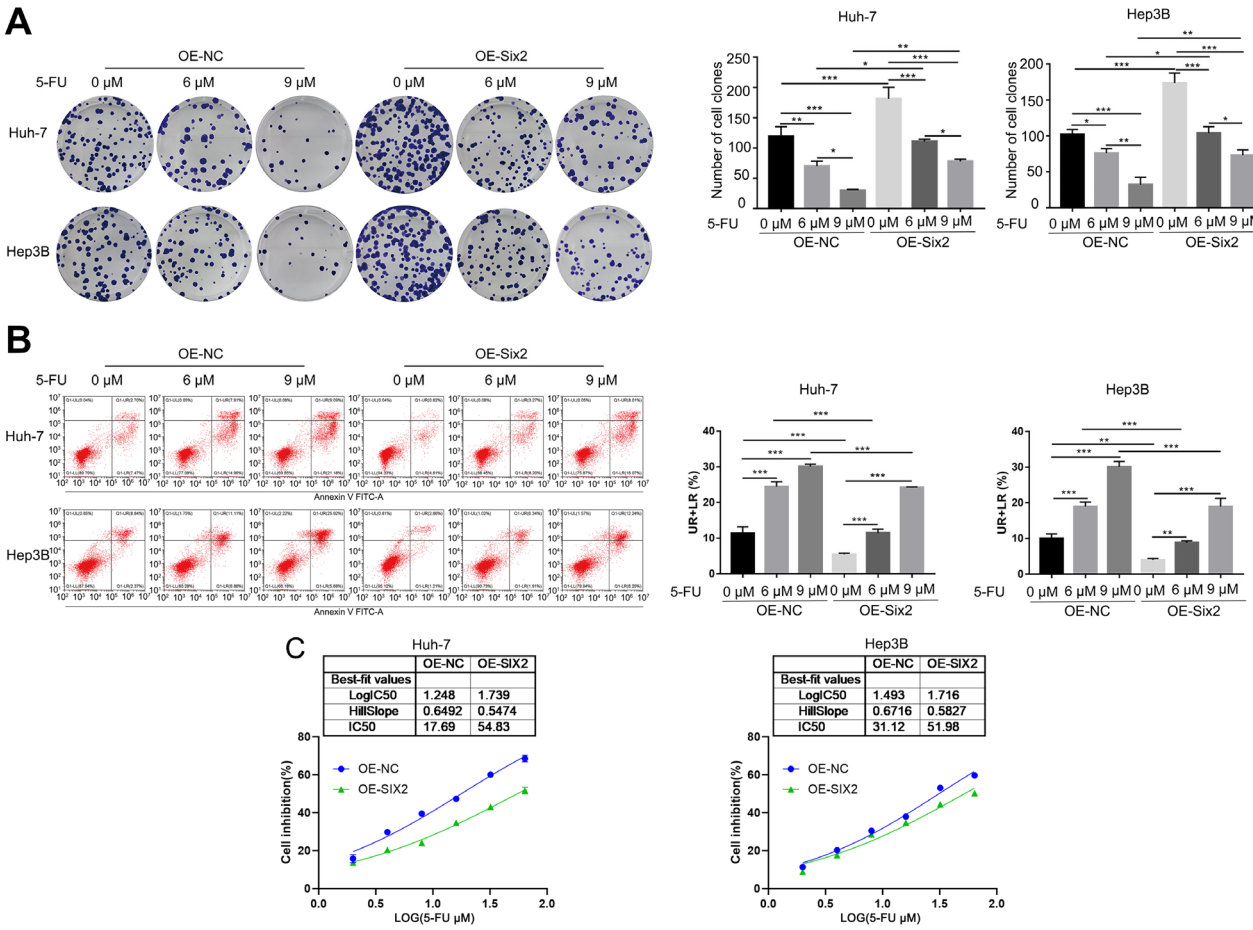

Figure 5. Six2 overexpression enhances resistance to 5-FU in Huh7 and Hep3B cells. A) Colony formation assay. B) Representative dot plots of cell apoptosis. C) IC_{50} assay of 5-FU. All experiments were performed with three biological replicates. Means ± SD *p<0.05, **p<0.01, ***p<0.001.

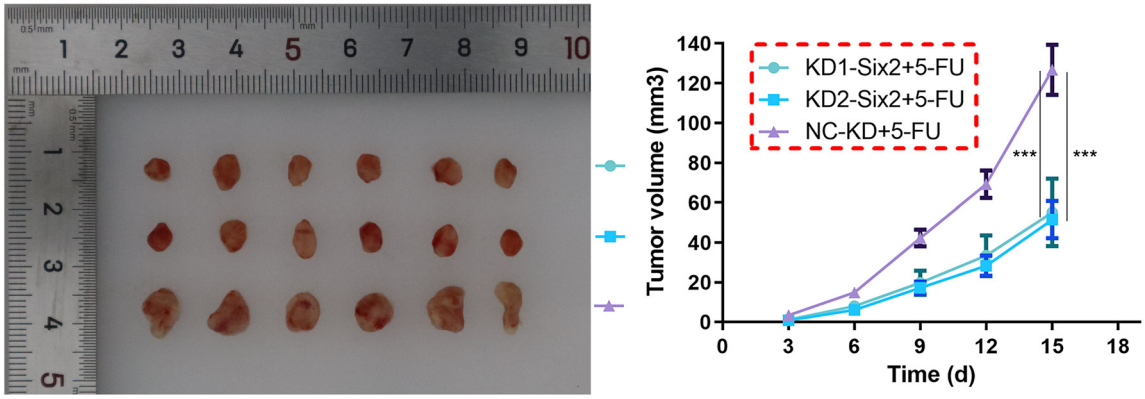

Figure 6. *In vivo* inhibition of Six2 expression enhances the 5-FU inhibitory effect on HCC cells in nude mice. All experiments were performed with six biological replicates. Means ± SD ***p<0.001.

and reduced nephron number [32]. Recently, growing evidence has highlighted the fundamental role of *Six2* in the initiation of carcinogenesis [33, 34]. Here, we observed that *Six2* knockdown markedly suppressed the growth, proliferation, invasion, and migration of HCC cells and potentiated 5-FU inhibitory effect, whereas *Six2* overexpression exerted opposite effects. These findings are consistent with previous reports about the effects of *Six2* on tumor cells

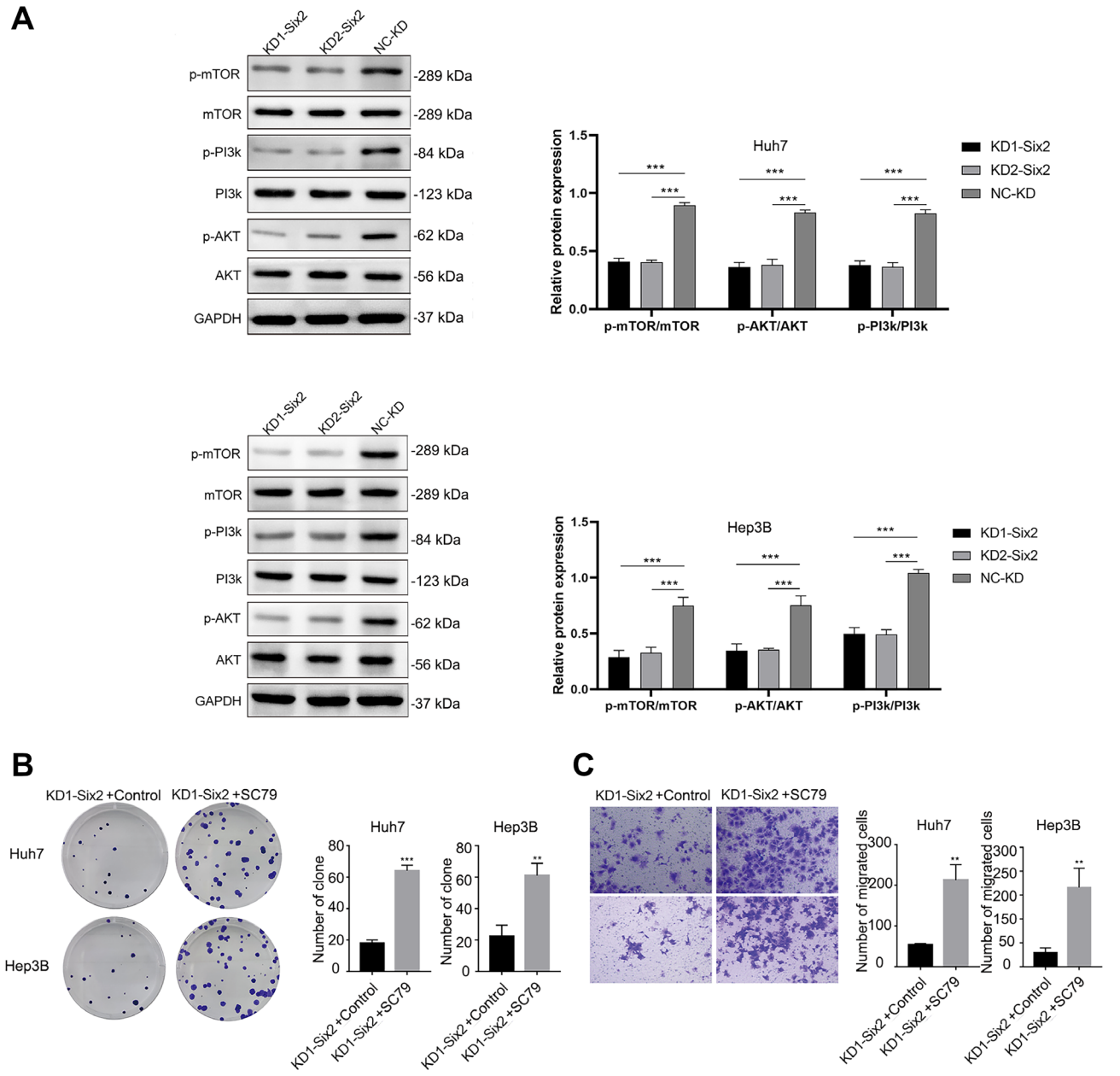

Figure 7. Six2 facilitates the proliferation and invasion of Huh7 and Hep3B cells through the PI3K/Akt/mTOR pathway. A) Western blot analysis of PI3K/Akt/mTOR pathway protein expression. B) Colony formation assay. C) Transwell invasion assay. All experiments were performed with three biological replicates. Means ± SD *p<0.05, **p<0.01, ***p<0.001.

[34–36]. Our results further affirm the crucial roles of *Six2* in tumor progression, highlighting its potential as a valuable biomarker and therapeutic target for the diagnosis and treatment of cancer.

Mechanistically, the Six gene family contributes to the induction of EMT by upregulating mesenchymal-related genes and downregulating epithelial-related genes, thereby promoting tumorigenesis [37, 38]. The loss of E-cadherin, an epithelial marker, is widely considered a hallmark of EMT [39]. Our previous work revealed that elevated Six2 expression in HCC reduces E-cadherin expression via enhancing methylation of the promoter [4]. Subsequently, this phenomenon has been demonstrated in other cancer types as well [19, 40]. In this study, we provide evidence that knockdown of *Six2* decreases CpG methylation, while upregulation of *Six2* increases CpG methylation of E-cadherin in HCC cells.

The above results suggested that *Six2*-mediated silencing of E-cadherin through methylation represents a fundamental phenomenon in cancer, underscoring the crucial role of *Six2* in tumor progression.

Downregulation of E-cadherin in human cancer is primarily achieved through DNA methylation [41]. However, the mechanisms by which Six2 contributes to the methylation of the E-cadherin promoter region remain unclear. Mammals possess three DNMT enzymes, namely DNMT1, DNMT3α, and DNMT3β, all of which share a highly conserved DNMT domain structure but exhibit distinct functions based on genetic and biochemical studies [42, 43]. DNMT1 has a strong preference for hemimethylated DNA and plays a crucial role in maintaining genomic methylation patterns [44]. Hypermethylation of tumor suppressor genes has been linked to tumorigenesis-associated DNMT1 activity, making it a potential target for cancer therapy [45]. It is noteworthy that the knockdown of *Six2* results in a decreased expression of DNMT1, whereas overexpression of Six2 induces elevated levels of DNMT1. This suggests that Six2 promotes DNMT1 expression in HCC cells, indicating a positive correlation between the expression of Six2 and DNMT1. Furthermore, ChIP-qPCR experiments confirmed that *Six2* knockdown inhibited DNMT1 binding to the E-cadherin promoter region. In summary, Six2 promotes methylation of the E-cadherin promoter region via its stimulation of DNMT1 activity, thereby facilitating HCC progression. These results highlight the potential of Six2 as a candidate for prognostic markers and therapeutic targets in HCC. Nevertheless, the underlying mechanisms by which Six2 affects DNMT1 activity require further exploration in a tightly controlled study.

The PI3K/Akt/mTOR pathway is an intracellular signaling pathway that plays a crucial role in regulating the cell cycle [46]. Aberrant activation of the PI3K/Akt/mTOR pathway is frequently observed in HCC, which has led to the clinical application of mTOR-targeting drugs such as RAD001 (everolimus) and rapamycin for HCC treatment [22]. However, the therapeutic efficacy of these targeted drugs is generally limited, which may be attributed to the feedback activation of AKT following mTOR inhibition [47]. Numerous studies have demonstrated that the suppression of the PI3K/Akt/mTOR signaling pathway can promote E-cadherin expression, thereby inhibiting EMT [48–50]. In the present study, we discovered that *Six2* knockdown inhibits HCC cell proliferation and invasion by suppressing the PI3K/Akt/mTOR pathway. Based on these findings and the relevant literature, we hypothesize that Six2 may promote HCC proliferation, invasion, and 5-FU resistance by activating the PI3K/Akt/mTOR signaling pathway. This activation could enhance DNMT1 expression and E-cadherin promoter methylation, ultimately facilitating E-cadherin transcription.

However, this study has certain limitations: 1) Notably, it lacks analysis of clinical samples. It is imperative to further evaluate the clinical significance of Six2 by analyzing its expression in HCC patient samples and correlating this expression with 5-FU treatment responses. 2) The long-term effects and potential side effects of Six2 knockdown on hepatocytes have not been explored, which is crucial for assessing its viability as a potential therapeutic target. 3) The failure to perform an *in vitro* experiment with the addition of 5-FU in Six2-silenced cells is a limitation of this study. In future studies, we will conduct relevant *in vitro* experiments to verify the inhibitory effect of Six2 silencing combined with 5-FU at the cellular level. 4) Drug resistance is a multifaceted phenomenon, often involving multiple factors. In addition to Six2, other factors must be considered to comprehensively elucidate the mechanisms of 5-FU resistance.5) The xenograft experiment in nude mice lacks a control tumor group without 5-FU treatment, making it difficult to assess the independent inhibitory effect of 5-FU alone. Therefore, further investigation is required to clarify the specific contribution of Six2 knockdown and the mechanisms by which it enhances the effect of 5-FU in this combined treatment. 6) The experiments did not fully mimic the complex tumor microenvironment *in vivo*, and further validation in multiple HCC cell lines and *in vivo* models is needed. These aspects will be further investigated in our subsequent studies.

In conclusion, this study reveals a novel role for Six2 in the progression of HCC and resistance to 5-FU. Six2 exhibits oncogenic properties in HCC through DNMT1-mediated E-cadherin promoter methylation and PI3K/Akt/mTOR pathway activation, contributing to cell proliferation, invasion, and 5-FU resistance. Therefore, Six2 might serve as a potential therapeutic target for HCC treatment.

Acknowledgments: This work was supported by the National Natural Science Foundation of China (82060550) and the Medical Scientific Research Foundation of Hainan Province of China (1601320673A2001).

References

[1] ZHOU M, YI Y, LIU L, LIN Y, LI J et al. Polymeric micelles loading with ursolic acid enhancing anti-tumor effect on hepatocellular carcinoma. J Cancer 2019; 10: 5820–5831. https://doi.org/10.7150/jca.30865

[2] KAYA E, DANIEL MAZZOLINI G, YILMAZ Y, CANBAY A. Prevention of hepatocellular carcinoma and monitoring of high-risk patients. Hepatol Forum 2022; 3: 33–38. https://doi.org/10.14744/hf.2021.2021.0033

[3] BROWN ZJ, HEWITT DB, PAWLIK TM. Experimental drug treatments for hepatocellular carcinoma: clinical trial failures 2015 to 2021. Expert Opin Investig Drugs 2022; 31: 693–706. https://doi.org/10.1080/13543784.2022.2079491

[4] LI JW, HUANG CZ, LI JH, YUAN JH, CHEN QH et al. Six2 is negatively correlated with good prognosis and decreases 5-FU sensitivity via suppressing E-cadherin expression in hepatocellular carcinoma cells. Biomed Pharmacother 2018; 104: 204–210. https://doi.org/10.1016/j.biopha.2018.05.032

[5] DUVAL AP, TROQUIER L, DE SOUZA SILVA O, DEMARTINES N, DORMOND O. Diclofenac Potentiates Sorafenib-Based Treatments of Hepatocellular Carcinoma by Enhancing Oxidative Stress. Cancers 2019; 11: 1453. https://doi.org/10.3390/cancers11101453

[6] SIEGEL RL, MILLER KD, WAGLE NS, JEMAL A. Cancer statistics, 2023. CA Cancer J Clin 2023; 73: 17–48. https://doi.org/10.3322/caac.21763

[7] GUO J, YU Z, SUN D, ZOU Y, LIU Y et al. Two nanoformulations induce reactive oxygen species and immunogenetic cell death for synergistic chemo-immunotherapy eradicating colorectal cancer and hepatocellular carcinoma. Mol Cancer 2021; 20: 10. https://doi.org/10.1186/s12943-020-01297-0

[8] GOMES SA, HARE JM, RANGEL EB. Kidney-Derived c-Kit(+) Cells Possess Regenerative Potential. Stem Cells Transl Med 2018; 7: 317–324. https://doi.org/10.1002/sctm.17-0232

[9] LI C, LIU H, HU YC, LAN Y, JIANG R. Generation and characterization of Six2 conditional mice. Genesis 2020; 58: e23365. https://doi.org/10.1002/dvg.23365

[10] WANG C, WANG J, BORER JG, LI X. Embryonic origin and remodeling of the urinary and digestive outlets. PLoS One 2013; 8: e55587. https://doi.org/10.1371/journal.pone.0055587

[11] LIU J, JU P, ZHOU Y, ZHAO Y, XIE Y et al. Six2 Is a Coordinator of LiCl-Induced Cell Proliferation and Apoptosis. Int J Mol Sci 2016; 17: 1504. https://doi.org/10.3390/ijms17091504

[12] LEE MY. Embryonic Programs in Cancer and Metastasis-Insights From the Mammary Gland. Front Cell Dev Biol 2022; 10: 938625. https://doi.org/10.3389/fcell.2022.938625

[13] JIN Y, LI JL. Olfactomedin-like 3: possible functions in embryonic development and tumorigenesis. Chin Med J (Engl) 2019; 132: 1733–1738. https://doi.org/10.1097/CM9.0000000000000309

[14] WU DW, LIN PL, WANG L, HUANG CC, LEE H. The YAP1/SIX2 axis is required for DDX3-mediated tumor aggressiveness and cetuximab resistance in KRAS-wild-type colorectal cancer. Theranostics 2017; 7: 1114–1132. https://doi.org/10.7150/thno.18175

[15] SONG D, YUE L, WU G, MA S, GUO L et al. Assessment of promoter methylation and expression of SIX2 as a diagnostic and prognostic biomarker in Wilms' tumor. Tumour Biol 2015; 36: 7591–7598. https://doi.org/10.1007/s13277-015-3456-5

[16] WU Y, SONG T, LIU M, HE Q, CHEN L et al. PPARG Negatively Modulates Six2 in Tumor Formation of Clear Cell Renal Cell Carcinoma. DNA Cell Biol 2019; 38: 700–707. https://doi.org/10.1089/dna.2018.4549

[17] WAN ZH, MA YH, JIANG TY, LIN YK, SHI YY et al. Six2 is negatively correlated with prognosis and facilitates epithelial-mesenchymal transition via TGF-beta/Smad signal pathway in hepatocellular carcinoma. Hepatobiliary Pancreat Dis Int 2019; 18: 525–531. https://doi.org/10.1016/j.hbpd.2019.09.005

[18] KARICHEVA O, RODRIGUEZ-VARGAS JM, WADIER N, MARTIN-HERNANDEZ K, VAUCHELLES R et al. PARP3 controls TGFbeta and ROS driven epithelial-to-mesenchymal transition and stemness by stimulating a TG2-Snail-E-cadherin axis. Oncotarget 2016; 7: 64109–64123. https://doi.org/10.18632/oncotarget.11627

[19] HOU H, YU X, CONG P, ZHOU Y, XU Y et al. Six2 promotes non-small cell lung cancer cell stemness via transcriptionally and epigenetically regulating E-cadherin. Cell Prolif 2019; 52: e12617. https://doi.org/10.1111/cpr.12617

[20] SURIYAMURTHY S, BAKER D, TEN DIJKE P, IYENGAR PV. Epigenetic Reprogramming of TGF-β Signaling in Breast Cancer. Cancers 2019; 11: 726. https://doi.org/10.3390/cancers11050726

[21] SUBRAMANIAM D, THOMBRE R, DHAR A, ANANT S. DNA methyltransferases: a novel target for prevention and therapy. Front Oncol 2014; 4: 80. https://doi.org/10.3389/fonc.2014.00080

[22] GRABINSKI N, EWALD F, HOFMANN BT, STAUFER K, SCHUMACHER U et al. Combined targeting of AKT and mTOR synergistically inhibits proliferation of hepatocellular carcinoma cells. Mol Cancer 2012; 11: 85. https://doi.org/10.1186/1476-4598-11-85

[23] JILEK JL, TU MJ, ZHANG C, YU AM. Pharmacokinetic and Pharmacodynamic Factors Contribute to Synergism between Let-7c-5p and 5-Fluorouracil in Inhibiting Hepatocellular Carcinoma Cell Viability. Drug Metab Dispos 2020; 48: 1257–1263. https://doi.org/10.1124/dmd.120.000207

[24] PERCIE DU SERT N, HURST V, AHLUWALIA A, ALAM S, AVEY MT et al. The ARRIVE guidelines 2.0: Updated guidelines for reporting animal research. Br J Pharmacol 2020; 177: 3617–3624. https://doi.org/10.1111/bph.15193

[25] NATIONAL RESEARCH COUNCIL COMMITTEE FOR THE UPDATE OF THE GUIDE FOR THE C, USE OF LABORATORY A. The National Academies Collection: Reports funded by National Institutes of Health. Guide for the Care and Use of Laboratory Animals. Washington (DC): National Academies Press (US) Copyright © 2011, National Academy of Sciences; 2011.

[26] WANG X, CHEN Y, DONG K, MA Y, JIN Q et al. Effects of FER1L4-miR-106a-5p/miR-372-5p-E2F1 regulatory axis on drug resistance in liver cancer chemotherapy. Mol Ther Nucleic Acids 2021; 24: 449–461. https://doi.org/10.1016/j.omtn.2021.02.006

[27] YOU MH, KIM WJ, SHIM W, LEE SR, LEE G et al. Cytosine deaminase-producing human mesenchymal stem cells mediate an antitumor effect in a mouse xenograft model. J Gastroenterol Hepatol 2009; 24: 1393–400. https://doi.org/10.1111/j.1440-1746.2009.05862.x

[28] LI H, SHENG C, LIU H, WANG S, ZHAO J et al. Inhibition of HBV Expression in HBV Transgenic Mice Using AAV-Delivered CRISPR-SaCas9. Front Immunol 2018; 9: 2080. https://doi.org/10.3389/fimmu.2018.02080

[29] XIE D, SHI J, ZHOU J, FAN J, GAO Q. Clinical practice guidelines and real-life practice in hepatocellular carcinoma: A Chinese perspective. Clin Mol Hepatol 2023; 29: 206–216. https://doi.org/10.3350/cmh.2022.0402

[30] XU J, LIU H, PARK JS, LAN Y, JIANG R. Osr1 acts downstream of and interacts synergistically with Six2 to maintain nephron progenitor cells during kidney organogenesis. Development 2014; 141: 1442–1452. https://doi.org/10.1242/dev.103283
[31] LITTLE MH, KAIRATH P. Does Renal Repair Recapitulate Kidney Development? J Am Soc Nephrol 2017; 28: 34–46. https://doi.org/10.1681/ASN.2016070748
[32] FOGELGREN B, YANG S, SHARP IC, HUCKSTEP OJ, MA W et al. Deficiency in Six2 during prenatal development is associated with reduced nephron number, chronic renal failure, and hypertension in Br/+ adult mice. Am J Physiol Renal Physiol 2009; 296: F1166–1178. https://doi.org/10.1152/ajprenal.90550.2008
[33] XU HX, WU KJ, TIAN YJ, LIU Q, HAN N et al. Expression profile of SIX family members correlates with clinic-pathological features and prognosis of breast cancer: A systematic review and meta-analysis. Medicine (Baltimore) 2016; 95: e4085. https://doi.org/10.1097/MD.0000000000004085
[34] JIANG Y, ZHOU B, LIANG B, ZENG F, ZOU Z. Overexpression of Sine Oculis Homeobox Homolog 2 Predicts Poor Survival and Clinical Parameters of Patients with Colon Adenocarcinoma. Ann Clin Lab Sci 2020; 50: 717–725.
[35] LIU Q, LI A, TIAN Y, LIU Y, LI T et al. The expression profile and clinic significance of the SIX family in non-small cell lung cancer. J Hematol Oncol 2016; 9: 119. https://doi.org/10.1186/s13045-016-0339-1
[36] CICERI S, MONTALVAO-DE-AZEVEDO R, TAJBAKHSH A, BERTOLOTTI A, SPAGNUOLO RD et al. Analysis of the mutational status of SIX1/2 and microRNA processing genes in paired primary and relapsed Wilms tumors and association with relapse. Cancer Gene Ther 2021; 28: 1016–1024. https://doi.org/10.1038/s41417-020-00268-3
[37] XU H, ZHANG Y, ALTOMARE D, PENA MM, WAN F et al. Six1 promotes epithelial-mesenchymal transition and malignant conversion in human papillomavirus type 16-immortalized human keratinocytes. Carcinogenesis 2014; 35: 1379–1388. https://doi.org/10.1093/carcin/bgu050
[38] MCCOY EL, IWANAGA R, JEDLICKA P, ABBEY NS, CHODOSH LA et al. Six1 expands the mouse mammary epithelial stem/progenitor cell pool and induces mammary tumors that undergo epithelial-mesenchymal transition. J Clin Invest 2009; 119: 2663–2677. https://doi.org/10.1172/JCI37691
[39] LAMOUILLE S, XU J, DERYNCK R. Molecular mechanisms of epithelial-mesenchymal transition. Nat Rev Mol Cell Biol 2014; 15: 178–196. https://doi.org/10.1038/nrm3758
[40] WANG CA, DRASIN D, PHAM C, JEDLICKA P, ZABER-EZHNYY V et al. Homeoprotein Six2 promotes breast cancer metastasis via transcriptional and epigenetic control of E-cadherin expression. Cancer Res 2014; 74: 7357–7370. https://doi.org/10.1158/0008-5472.CAN-14-0666
[41] WANG ZY, LU J, ZHANG YZ, ZHANG M, LIU T et al. Effect of Bisphenol A on invasion ability of human trophoblastic cell line BeWo. Int J Clin Exp Pathol 2015; 8: 14355–14364.
[42] GABBIANELLI R, BORDONI L, MORANO S, CALLEJA-AGIUS J, LALOR JG. Nutri-Epigenetics and Gut Microbiota: How Birth Care, Bonding and Breastfeeding Can Influence and Be Influenced? Int J Mol Sci 2020; 21: 5032. https://doi.org/10.3390/ijms21145032
[43] LEPPERT S, MATARAZZO MR. De novo DNMTs and DNA methylation: novel insights into disease pathogenesis and therapy from epigenomics. Curr Pharm Des 2014; 20: 1812–1818. https://doi.org/10.2174/13816128113199990534
[44] QI X, YU XJ, WANG XM, SONG TN, ZHANG J et al. Knockdown of KCNQ1OT1 Suppresses Cell Invasion and Sensitizes Osteosarcoma Cells to CDDP by Upregulating DNMT1-Mediated Kcnq1 Expression. Mol Ther Nucleic Acids 2019; 17: 804–818. https://doi.org/10.1016/j.omtn.2019.06.010
[45] BASHTRYKOV P, JELTSCH A. DNMT1-associated DNA methylation changes in cancer. Cell Cycle 2015; 14: 5. https://doi.org/10.4161/15384101.2014.989963
[46] TEWARI D, PATNI P, BISHAYEE A, SAH AN, BISHAYEE A. Natural products targeting the PI3K-Akt-mTOR signaling pathway in cancer: A novel therapeutic strategy. Semin Cancer Biol 2022; 80: 1–17. https://doi.org/10.1016/j.semcancer.2019.12.008
[47] FINN RS. Current and Future Treatment Strategies for Patients with Advanced Hepatocellular Carcinoma: Role of mTOR Inhibition. Liver Cancer 2012; 1: 247–256. https://doi.org/10.1159/000343839
[48] JIA M, QIU H, LIN L, ZHANG S, LI D et al. Inhibition of PI3K/AKT/mTOR Signalling Pathway Activates Autophagy and Suppresses Peritoneal Fibrosis in the Process of Peritoneal Dialysis. Front Physiol 2022; 13: 778479. https://doi.org/10.3389/fphys.2022.778479
[49] LIAO H, ZHANG L, LU S, LI W, DONG W. KIFC3 Promotes Proliferation, Migration, and Invasion in Colorectal Cancer via PI3K/AKT/mTOR Signaling Pathway. Front Genet 2022; 13: 848926. https://doi.org/10.3389/fgene.2022.848926
[50] YUAN R, FAN Q, LIANG X, HAN S, HE J et al. Cucurbitacin B inhibits TGF-β1-induced epithelial-mesenchymal transition (EMT) in NSCLC through regulating ROS and PI3K/Akt/mTOR pathways. Chin Med 2022; 17: 24. https://doi.org/10.1186/s13020-022-00581-z